Biochimica et Biophysica Acta 1842 (2014) 2163–2173

Contents lists available at ScienceDirect

Biochimica et Biophysica Acta

journal homepage: www.elsevier.com/locate/bbadis

FAD binding overcomes defects in activity and stability displayed by cancer-associated variants of human NQO1

Angel L. Pey [a,*], Clare F. Megarity [b], David J. Timson [b,c,**]

[a] Department of Physical Chemistry, Faculty of Sciences, University of Granada, Av. Fuentenueva s/n, 18071, Spain
[b] School of Biological Sciences, Queen's University Belfast, Medical Biology Centre, 97 Lisburn Road, Belfast BT9 7BL, UK
[c] Institute for Global Food Security, Queen's University Belfast, 18-30 Malone Road, Belfast BT9 5BN, UK

ARTICLE INFO

Article history:
Received 11 June 2014
Received in revised form 8 August 2014
Accepted 20 August 2014
Available online 29 August 2014

Keywords:
NAD(P)H quinone oxidoreductase 1
Cancer-associated polymorphism
NQO1*2
NQO1*3
Kinetic instability

ABSTRACT

NAD(P)H quinone oxidoreductase 1 is involved in antioxidant defence and protection from cancer, stabilizing the apoptosis regulator p53 towards degradation. Here, we studied the enzymological, biochemical and biophysical properties of two cancer-associated variants (p.R139W and p.P187S). Both variants (especially p.187S) have lower thermal stability and greater susceptibility to proteolysis compared to the wild-type. p.P187S also has reduced activity due to a lower binding affinity for the FAD cofactor as assessed by activity measurements and direct titrations. Native gel electrophoresis and dynamic light scattering also suggest that p.P187S has a higher tendency to populate unfolded states under native conditions. Detailed thermal stability studies showed that all variants irreversibly denature causing dimer dissociation, while addition of FAD restores the stability of the polymorphic forms to wild-type levels. The kinetic destabilization induced by polymorphisms as well as the kinetic protection exerted by FAD was confirmed by measuring denaturation kinetics at temperatures close to physiological. Our data suggest that the main molecular mechanisms associated with these cancer-related variants are their low binding affinity for FAD and/or kinetic instability. Thus, pharmacological chaperones may be useful in the treatment of patients bearing these polymorphisms.

1. Introduction

NAD(P)H quinone oxidoreductase 1 (NQO1, DT-diaphorase, EC 1.6.5.2) is a mammalian enzyme which catalyses the two electron reduction of quinones and related substrates. The enzyme belongs to a family which also contains mammalian dihydronicotinamide riboside (NRH) quinone oxidoreductase 2 (NQO2, EC 1.10.99.2) and bacterial enzymes such as MdaB [1–3]. The family members are typically dimeric and have an FAD cofactor bound to each subunit [4–7]. They catalyse the reduction of quinones (and related compounds) through a substituted enzyme ("ping-pong") mechanism in which NAD(P)H (or NRH in the case of NQO2) enters the active site, reduces the FAD and exits as the oxidised form. The second substrate then enters the active site and is reduced by the $FADH_2$ [1,8,9].

There appear to be several physiological roles for NQO1. Its enzymatic function has a minor role in vitamin K metabolism [10,11]. More generally, the enzyme catalyses the two electron reduction of quinone substrates, helping maintain the vitamin E derivative α-tocopherol quinone and ubiquinone (coenzyme Q) in their reduced, antioxidant forms [12,13]. The two electron reduction mechanism avoids the production of semiquinones [14]. These compounds are highly reactive and can induce the production of reactive oxygen species in the cell. However, the protein also has non-catalytic roles. In its reduced state, it binds to the apoptosis regulating protein p53 and stabilizes it [15,16]. It also binds to the tumour suppressor protein p73 and the polyamine biosynthesis pathway enzyme ornithine decarboxylase [17,18]. NQO1 interacts with the 20S proteasome reducing its activity, preventing it from degrading these proteins; however, partially unfolded forms of NQO1 can be efficiently degraded by the 20S proteasome [19].

NQO1 is implicated in the molecular pathology of some cancers. The amount of the enzyme is increased in some colon, liver, breast and lung tumours [20]. Consequently it has attracted interest as a possible target for cancer chemotherapy [21–24]. There are also some anticancer pro-drugs (e.g. mitomycin C (MMC) and a MMC analogue, EO9) which are reduced by NQO1 to the active form [25–27]. Interestingly there are two polymorphic forms of NQO1 which are associated with higher cancer risks. The first one to be characterized, rs1800566 (c.C609T), is sometimes known as the NQO1*2 allele [28,29]. Globally

Abbreviations: BS^3, *bis*sulfosuccinimidyl-suberate; CD, circular dichroism; EDC, *N*-(3-dimethylaminopropyl)-*N*′-ethylcarbodiimide hydrochloride; DSC, differential scanning calorimetry; DSF, differential scanning fluorimetry; ITC, isothermal titration calorimetry; MMC, mitomycin C; NQO1, NAD(P)H quinone oxidoreductase 1; NQO2, dihydronicotinamide riboside quinone oxidoreductase 2; T_m, melting temperature

* Corresponding author.
** Correspondence to: D.J. Timson, School of Biological Sciences, Queen's University Belfast, Medical Biology Centre, 97 Lisburn Road, Belfast BT9 7BL, UK.
E-mail addresses: angelpey@ugr.es (A.L. Pey), d.timson@qub.ac.uk (D.J. Timson).

http://dx.doi.org/10.1016/j.bbadis.2014.08.011
0925-4439/

the frequency of this allele in the human population is estimated to be 28%, rising to 51% in Han Chinese people (http://www.ensembl.org/Homo_sapiens/Variation/Population?db=core;r=16:69744645-69745645;v=rs1800566;vdb=variation;vf=1369178) [30]. It results in a proline to serine substitution at position 187 in the polypeptide sequence. Biochemically it is associated with reduced cellular NQO1 protein levels [29]. Cells homozygous for this polymorphism have undetectable levels of NQO1 activity [29,31]. The reduction in activity also means that reductive activation of drugs such as MMC is less efficient and so cells expressing this variant form of NQO1 are less responsive to these compounds [28]. The p.P187S variant is highly susceptible to degradation by the 20S proteasome [19,32]. A large number of epidemiological studies have demonstrated that this allele is associated with increased cancer risks, although some question its significance — for recent examples, see [33–38]. Smokers who are homozygous for this mutation have an even greater risk of lung cancer than those who have at least one wild-type allele [39,40]. Homozygotes also have an increased susceptibility to benzene toxicity [41–43].

A second allele, NQO1*3 (rs1131341, c.C465T), is less well studied [44,45]. It results in an arginine to tryptophan substitution at position 139. The global frequency of this allele is estimated to 2% with the highest known frequency (7%) in the Spanish Iberian population (http://www.ensembl.org/Homo_sapiens/Variation/Population?db=core;r=16:69748369-69749369;v=rs1131341;vdb=variation;vf=888801) [30]. p.R139W has also been associated with cancer, specifically childhood acute lymphoblastic leukaemia [46,47]. Reduced responsiveness to MMC has also been reported [44,45]. Arginine 139 is positioned within the large catalytic domain on the periphery of the enzyme; it is in a loop and is solvent exposed. Proline 187 is also positioned in a loop within the large catalytic domain and although more buried that arginine 139, is still solvent accessible. Neither residue forms part of the enzyme's active site (Fig. 1).

To better understand the fundamental molecular pathology of these two alleles, we expressed and purified the corresponding recombinant proteins, providing unprecedented detail on the effects of p.P187S and characterizing for the first time the effects of p.R139W at the molecular level. This enabled us to propose that their reduced enzymatic activity results from protein instability (relative to the wild-type) and to investigate the role of FAD-mediated stabilization of NQO1. Our studies also provide a framework for the design of therapies aimed to rescue NQO1 functionality in patients bearing these polymorphisms.

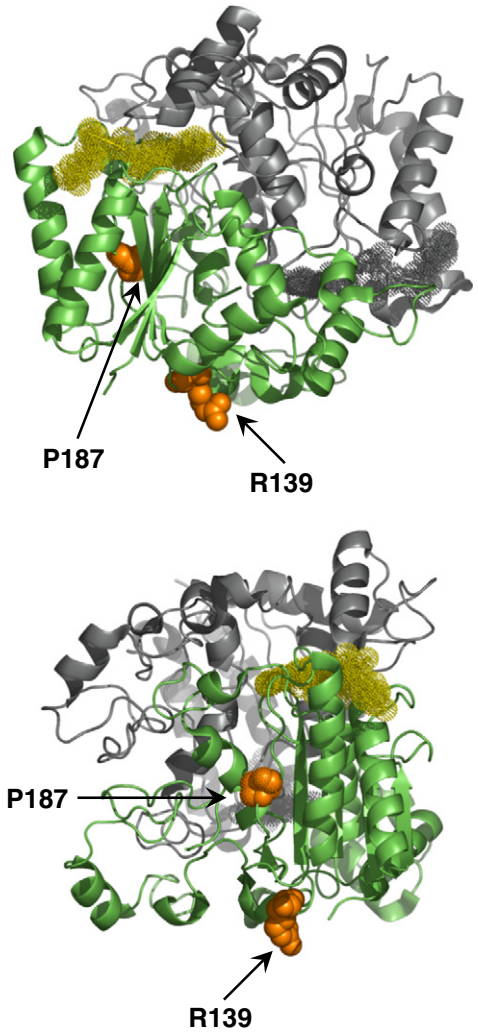

Fig. 1. Structure of human NQO1 showing the location of Arg139 and Pro187. One monomer of the NQO1 dimer is shown in green, with the FAD cofactor in yellow and the two residues in green; the other monomer is shown in grey. In both orientations depicted, the active site lies above the FAD molecule. The lower image shows the protein rotated 90° around the y-axis relative to the upper one. The figure was constructed using data from PDB ID 2F1O [5] and PyMol (www.pymol.org).

2. Materials and methods

2.1. Expression and purification of wild-type and variant NQO1

Hexahistidine-tagged human NQO1 was expressed in, and purified from, *Escherichia coli* cells. The coding sequence for human *NQO1* was amplified from I.M.A.G.E. clone 3349257 [48] and inserted into the *E. coli* expression vector pET46 Ek/LIC (Merck, Nottingham, UK). Site-directed mutagenesis was carried out using the QuikChange method [49]. All coding sequences were verified by DNA sequencing (GATC Biotech, London, UK). Competent *E. coli* HMS174 (DE3) cells were transformed with the appropriate plasmid; a single colony resulting from this transformation was selected and grown shaking (200 rpm) at 37 °C overnight in 5 ml of LB supplemented with ampicillin (100 μg ml^{-1}). This culture was diluted into 1 l of LB supplemented with ampicillin (100 μg ml^{-1}) and grown until mid-log phase (~4 h). The culture was induced by the addition of IPTG (1.7 mM) and grown for a further 3–4 h. The culture was centrifuged at 4200 *g* at 4 °C for 15 min, the pellets were resuspended in cold buffer R (50 mM Hepes–NaOH, pH 7.5, 150 mM NaCl, 10%(v/v) glycerol) and stored, frozen, at −80 °C. Cells were thawed and disrupted by sonication on ice (3 × 30 s pulses at 100 W with 30 s intervals). Insoluble material was removed by centrifugation (27,000 *g*, 20 min at 4 °C). The supernatant was applied to a nickel agarose resin column (1 ml, His-Select™ Ni^{2+} affinity gel, Sigma-Aldrich) which had been pre-equilibrated with buffer A (buffer R, except 500 mM NaCl) and was allowed to pass through under gravity. The column was washed with 50 ml of buffer A and the protein was eluted from the column by administration of two 2 ml volumes of buffer A supplemented with 250 mM imidazole. Fractions containing NQO1 were identified by SDS PAGE and were dialysed overnight against 1 l of buffer R supplemented with 1 mM DTT at 4 °C. The protein concentration was determined by the method of Bradford [50] and aliquots (50–100 μl) were stored at −80 °C. At least four independent purifications were performed for each of the NQO1 variants, and several control experiments were carried out to confirm that key results are batch-independent. The dimeric nature of NQO1 enzymes was routinely checked by size-exclusion chromatography on HiLoad 16/60 Superdex 200 column (GE Healthcare).

For spectroscopic and calorimetric studies, protein concentration was measured using extinction coefficients based on the primary sequences (wild-type and p.P187S, $\varepsilon_{280\ nm} = 47{,}900\ M^{-1} \cdot cm^{-1}$; p.R139W, $\varepsilon_{280\ nm} = 53{,}400\ M^{-1} \cdot cm^{-1}$). Spectra of wild-type and R139W were corrected for the absorbance of FAD bound during purification (using $\varepsilon_{280\ nm} = 22{,}000\ M^{-1} \cdot cm^{-1}$ and $\varepsilon_{450\ nm} = 11{,}300\ M^{-1} \cdot cm^{-1}$ for free FAD). FAD was removed from NQO1 variants by performing dilution/concentration cycles in 2 M KBr, 50 mM

Hepes–KOH pH 7.4 using 30 kDa cut-off filters and in this case their spectra were not corrected due to the FAD bound. The samples were considered to be FAD free when the $A_{280}/A_{450} > 200$, buffer exchanged to 50 mM Hepes–KOH pH 7.4 and stored at −80 °C. FAD was dissolved in 50 mM HEPES–KOH pH 7.4 and its concentration was measured using $\varepsilon_{450\ nm} = 11{,}300\ M^{-1} \cdot cm^{-1}$.

2.2. Enzyme kinetics

NQO1 activity was measured in either 50 mM phosphate buffer pH 7.4 or 50 mM HEPES–NaOH pH 7.33 using NADH or NADPH as the electron donor and DCPIP (70 μM) as the electron acceptor; lysozyme (0.9 μM, Sigma) was included as a stabilizing agent. Initial reaction rates were determined from changes in $A_{600\ nm}$ resulting from the reduction of DCPIP and correcting for the non-enzymatic rate of DCPIP reduction. All reactions were carried out in triplicate in a reaction volume of 150 μl in 96-well plates at 37 °C in a Multiskan Spectrum plate reader (Thermo Scientific). Enzyme concentration was kept low enough to provide reliable estimations of changes in $A_{600\ nm}$. To determine the effect of FAD on the rate of reaction catalysed by the p.P187S variant, aliquots of the protein (400 nM) were mixed with FAD (1–64 μM) and incubated on ice for ~5 min. The enzyme was then diluted into the assay mix so that the final concentration of protein was 4 nM and the FAD concentration ranged from 10 to 640 nM. Control experiments in the absence of protein were also carried out.

The apparent Michaelis constant ($K_{m,app}$) and turnover number ($k_{cat,app}$) were determined from plots of enzyme-catalysed rate divided by enzyme concentration against the corresponding [NAD(P)H]. The data were fitted to Eq. (1) using non-linear curve fitting in GraphPad Prism 6.0 (GraphPad Software Inc., CA, USA).

$$v/[E] = k_{cat,app}[NAD(P)H]/K_{m,app} + [NAD(P)H] \quad (1)$$

where $k_{cat,app}$ is the apparent turnover number; $K_{m,app}$ is the apparent Michaelis–Menten constant; [E] is the concentration of enzyme dimer. Control experiments demonstrated that there was a linear relationship between the rate and the enzyme concentration in the range used in these experiments (data not shown). Possible cooperative response to NADH or NADPH concentration was evaluated by analysis using linearized Hill plots.

2.3. Tris–glycine native PAGE

Wild type and variant enzymes were diluted to a final concentration of 3 μM dimer. An equal volume of native gel loading buffer (125 mM Tris–HCl, pH 8.8; 20% (v/v) glycerol; 1% (w/v) DTT; 0.002% (w/v) bromophenol blue) was added and the samples were loaded onto a 10% native polyacrylamide gel (stacking gel pH 6.8; resolving gel pH 8.8) and electrophoresed at 20 mA until the dye in the front reached the end of the gel. Gels were stained with Coomassie Blue.

2.4. Crosslinking

Increasing concentrations of the chemical cross-linkers *bis*sulfosuccinimidyl-suberate (BS^3) and *N*-(3-Dimethylaminopropyl)-*N*′-ethylcarbodiimide hydrochloride (EDC) were added to a constant concentration of NQO1 and variants (5 μM dimer in buffer R) which had been preincubated for 15 min at 37 °C. The reaction was allowed to proceed for 30 min at 37 °C after which time it was stopped by the addition of SDS loading buffer (0.122 M Tris (pH 6.8); 4% (w/v) SDS; 19.5% (v/v) Glycerol; 0.13 M DTT; Bromophenol Blue 0.05% (w/v)). Reactions were analyzed using SDS PAGE.

2.5. Limited proteolysis

Increasing concentrations of trypsin were added to samples of each NQO1 variant (3.5 μM dimer in buffer R). Proteolysis was allowed to proceed for 30 min at 37 °C and was stopped by the addition of SDS Tris–tricine loading buffer (12% SDS (w/v); 6% DTT (w/v); 30% Glycerol; 150 mM Tris–HCl pH 7; 0.05% Bromophenol Blue (w/v)). Samples were denatured by heating at 95 °C for 5 min and analyzed on 13% SDS Tris–tricine gels [51].

2.6. Differential scanning fluorimetry (DSF)

Wild-type NQO1, p.R139W and p.P187S were diluted to 2 μM (dimer), 2 μM (dimer) and 10 μM (dimer) respectively. The samples were loaded in triplicate into a Rotor-Gene Q cycler (Qiagen) and the high resolution melt protocol was selected. Proteins were subjected to an increase in temperature form 25 °C to 95 °C in 1 K increments (no gain optimisation selected). The fluorescence of the cofactor, FAD, was exploited by exciting at 460 nm and measuring emission at 510 nm [52,53]. The melting temperature (T_m) of each variant was determined from the first derivative of the melting curve.

2.7. Spectroscopic analyses

All spectroscopic analyses were performed in Hepes–KOH 50 mM pH 7.4 unless otherwise indicated. Circular dichroism (CD) measurements were performed in a Jasco J-710 spectropolarimeter using 1 mm (Far-UV) or 5 mm (Near-UV/visible) path-length cuvettes. Thermal and wavelength scans were acquired using 5 (Far-UV, in K-phosphate 50 mM pH 7.4) or 10 μM (Near-UV/visible) NQO1. Thermal scans by far-UV CD were registered at 222 nm from 10 to 80 °C at a 2 K/min scan rate, and the apparent T_m values were estimated as the maxima of the first derivative of thermal scans. In some cases, FAD was added to a final concentration up to 0.25 mM. Fluorescence spectra were acquired in a Cary Eclipse spectrofluorometer using 3 mm path length cuvettes. All spectra were acquired at 25 °C at a 50–100 nm/min scan rates and 4–6 scans were registered and averaged. Dynamic light scattering (DLS) was carried out in a DynaPro MSX instrument (Wyatt) using 1.5 mm path length cuvettes and 5–10 μM protein (monomer). Fifty spectra were acquired for each DLS analysis, averaged and used to determine the hydrodynamic radius (assuming a spherical particle shape) and polydispersity using the average autocorrelation function.

To monitor isothermal denaturation of NQO1 variants, 230 μl of 50 mM Hepes–KOH pH 7.4 in the presence of 0–250 μM FAD was incubated at 37 °C or 42 °C for 10 min and then 20 μl of NQO1 enzymes (~90 μM monomer) incubated with 0–250 μM FAD was added and manually mixed (dead time between 10 and 60 s). The ellipticity at 222 nm was registered as a function of time for up to 50 h. To determine the apparent half-life for denaturation, kinetic traces were analyzed using a single exponential function.

2.8. Differential scanning calorimetry (DSC)

DSC studies were performed on a capillary VP-DSC differential scanning calorimeter (MicroCal, GE Healthcare) with a cell volume of 0.135 ml. Scans were performed at a 1–3 K/min in a temperature range of 5–80 °C using 5–30 μM NQO1 (monomer) in 50 mM HEPES–KOH, pH 7.4. In some experiments, FAD was added to a final concentration up to 0.5 mM.

Thermal denaturation of NQO1 variants was analyzed using a phenomenological two-state irreversible denaturation model with non-first order kinetics [54–56], depicted by (Scheme 1):

$$N_\mu \xrightarrow[k]{} F$$

where N_μ is the native oligomeric ensemble of NQO1 (i.e. a dimer with different number of FAD molecules bound/dimer), F an irreversibly aggregated state that cannot fold back, k is the rate constant for its conversion and $1/\mu$ is the reaction order. Additional details on the analysis of DSC data can be found in the Supplementary Information.

2.9. Isothermal titration calorimetry (ITC)

Experiments were performed in a VP ITC_{200} microcalorimeter (GE Healthcare) with a cell volume of 0.206 ml. Cell samples contained 5–6 μM NQO1 variants (dimer) in Hepes–KOH 50 mM pH 7.4 and were titrated using 0.25 mM FAD by performing 30–50 injections of 0.8–1.2 μl each 180–240 s. Data were corrected for heats of dilution by performing FAD titrations into buffer. After peak integration, binding isotherms were fitted using a sequential binding model with two binding sites or a one identical and independent type of sites model using the software provided by the manufacturer. Additional details on the analysis of ITC data can be found in the Supplementary Information.

3. Results

3.1. Expression, purification and dimerisation of wild-type and variant NQO1

Wild type human NQO1 could be expressed in, and purified from, *E. coli* with a typical yield of 5 mg per litre of culture. The variants p.R139W and p.P187S could also be expressed and purified albeit with slightly lower yields of 3 and 2 mg per litre of culture respectively (Supplementary Fig. S1a). Solutions of purified wild-type and p.R139W proteins were an intense yellow colour whereas p.P187S was not; this indicated that p.P187S had substantially less FAD bound. As expected, homodimers of the wild-type protein were detected by protein–protein crosslinking with both EDC and BS^3 and size-exclusion chromatography. Both variants also formed homodimers (Supplementary Fig. S1b,c,d). FAD (0–80 μM) had no effect on the amount of BS^3 crosslinking observed (data not shown).

3.2. Activity of wild-type and variant NQO1

Wild-type NQO1 and p.R139W were active with both NADH and NADPH as electron donors and DCPIP as the electron acceptor (Fig. 2; Table 1); p.P187S had no detectable activity under these conditions (data not shown). Pre-incubation of the enzyme with excess FAD prior to its addition to the reaction recovered the activity of p.P187S (Supplementary Fig. S2) and increased the activity of wild-type and p.R139W (data not shown). The kinetic constants for wild-type NQO1 and p.R139W are broadly similar; however, p.R139W is slightly more active with NADH than the wild-type as judged by the specificity constant (k_{cat}/K_m; note that this parameter is not dependent on concentration of fixed substrate in the substituted enzyme mechanism [57]). It has been reported previously that rat NQO1 exhibits negative cooperativity towards inhibitors which are competitive with respect to NAD(P)H [58]. Neither wild-type human NQO1 nor p.R139W exhibited cooperativity towards either NADH or NADPH (Supplementary Fig. S3; Table 1).

3.3. Protein conformation and FAD binding

As isolated, wild-type and p.R139W display similar hydrodynamic radii (3.60 ± 0.05 and 3.66 ± 0.15 nm, respectively). The hydrodynamic radius of p.P187S is slightly larger (4.06 ± 0.07 nm, $p < 0.01$ using a t-test vs. WT or p.R139W), suggesting that the ensemble average conformation of P187S is slightly expanded (Fig. 3A,B) possibly due to the presence of low levels of partially unfolded states. All three enzymes behave as monodisperse particles, with polydispersities in the range of ~10–15% (Fig. 3B). Interestingly, addition of FAD seems to slightly reduce the hydrodynamic size of p.P187S while having no significant effect on wild-type and p.R139W (Fig. 3A). Consistent with these effects on the overall conformation of p.R139W and p.P187S, the far-UV CD spectra in the absence or presence of 50 μM FAD revealed very similar secondary structure content in the three NQO1 variants (Fig. 3C). The tryptophan emission spectra of wild-type and p.R139W show the same maxima (λ_{max} = 352 nm) and the higher intensity of p.R139W can be easily explained by the extra tryptophan residue (wild-type NQO1 has six tryptophans), while the spectra of P187S have a λ_{max} of 348 nm and a higher fluorescence intensity, suggesting some changes

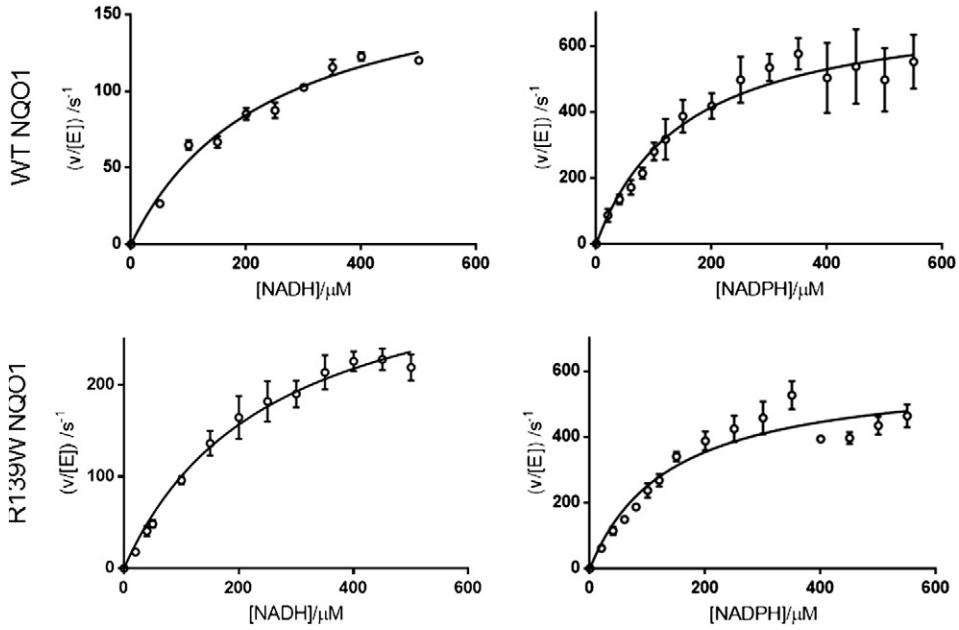

Fig. 2. Steady state enzyme kinetics for wild-type NQO1 and p.R139W. The dependence of rate on NADH and NADPH concentrations for wild-type NQO1 (top) and R139W (bottom) rates measured at 37 °C with 70 μM DCPIP and 3 nM (dimer) wild-type NQO1 and p.R139W for NADH and 1.5 nM (dimer) wild-type NQO1 and p.R139W for NADPH (0–350 μM) and 1.0 nM enzyme for NADPH (400–550 μM). Each point represents the mean of three separate determinations and the error bars are the standard errors of these means.

Table 1
Steady-state kinetic parameters for wild-type NQO1 and p.R139W.

	Wild-type NQO1		p.R139W NQO1	
	NADH	NADPH	NADH	NADPH
$K_{m,app}$/μM	240 ± 34	154 ± 38	256 ± 48	138 ± 24
$k_{cat,app}/s^{-1}$	186 ± 12*	732 ± 68	356 ± 31*	598 ± 37
$k_{cat}/K_m/\mu M^{-1}\ s^{-1}$	0.8 ± 0.2*	4.8 ± 1.6	1.4 ± 0.4*	4.3 ± 1.0
h	1.05 ± 0.05	1.10 ± 0.10	1.11 ± 0.04	1.14 ± 0.12

Rates measured at 37 °C with varying concentrations of electron donor (NADH or NADPH) and a constant concentration of electron acceptor, (DCPIP, 70 μM) background rates for the non-enzymatic reduction of DCPIP at each concentration of electron donor subtracted to give the enzyme catalysed rate. Values were derived from non-linear curve fitting of triplicate data. Values marked * are significantly different ($p < 0.05$; F-test) between the wild-type and p.R139W.

in the microenvironment of the tryptophan residues or lower quenching by the bound FAD molecules in this variant (Fig. 3D). In the course of the purifications, we noticed the faint yellow colour of p.P187S in contrast to the wild-type and p.R139W. Indeed, the absorption (Fig. 3E) and circular dichroism spectra (Fig. 3F) in the Near-UV visible region reveal signals corresponding to FAD bound (with maxima at ~370 and ~450 nm) in the wild-type and p.R139W, while in the spectra for P187S these signals are approximately 10-fold weaker (Fig. 3E,F).

To further characterize the binding of FAD to NQO1, we used isothermal titration calorimetry (ITC). FAD binding to apo-wild-type and p.R139W showed complex behaviour, which was not consistent with the presence of one type of identical and independent sites. Analyses of the isotherms using a sequential binding model with two binding sites provide excellent descriptions for FAD binding to wild-type and p.R139W enzymes (Fig. 4A). These analyses showed that K_1 far exceeds K_2 (20–60 fold), which is consistent with the presence of two independent and different types of sites or two identical and interacting types of sites displaying negative cooperativity (Table 2 and Supplemental information). In contrast, FAD binding to apo-p.P187S was well described by single type of independent and identical site (Fig. 4A), as shown by very good fits obtained to this model and the fact that $K_1 \approx 4 \cdot K_2$ in the sequential binding model (as expected for identical and independent sites, see Supplementary Material) (Table 2). This variant displayed between 10–1000 fold lower binding affinity than wild-type and p.R139W (Table 2). This lower affinity in p.P187S explains why the FAD bound to this variant is much lower in the recombinant protein as purified. Moreover, simulations of FAD binding as a function of its concentration showed that at physiological free FAD concentrations (58 nM [59]), the low affinity of p.P187S for FAD will result in a significant amount of apo-protein, which may be unstable intracellularly (Fig. 4B,C,D).

3.4. The cancer-associated variants are unstable compared to the wild-type

A common cause of loss of activity in disease-associated variants of proteins is reduced structural stability compared to the wild-type. In native gel electrophoresis, p.R139W ran further than wild-type NQO1, most likely because of the change in isoelectric point resulting from altering a positively charged arginine residue to uncharged tryptophan [45]. p.P187S ran as a smear on the native gel in comparison to the more discrete bands observed for wild-type and p.R139W (Fig. 5A). These results suggest that p.P187S is more prone to populate partially unfolded states consistent with our DLS analyses (Fig. 3A,B) and other previous results [19].

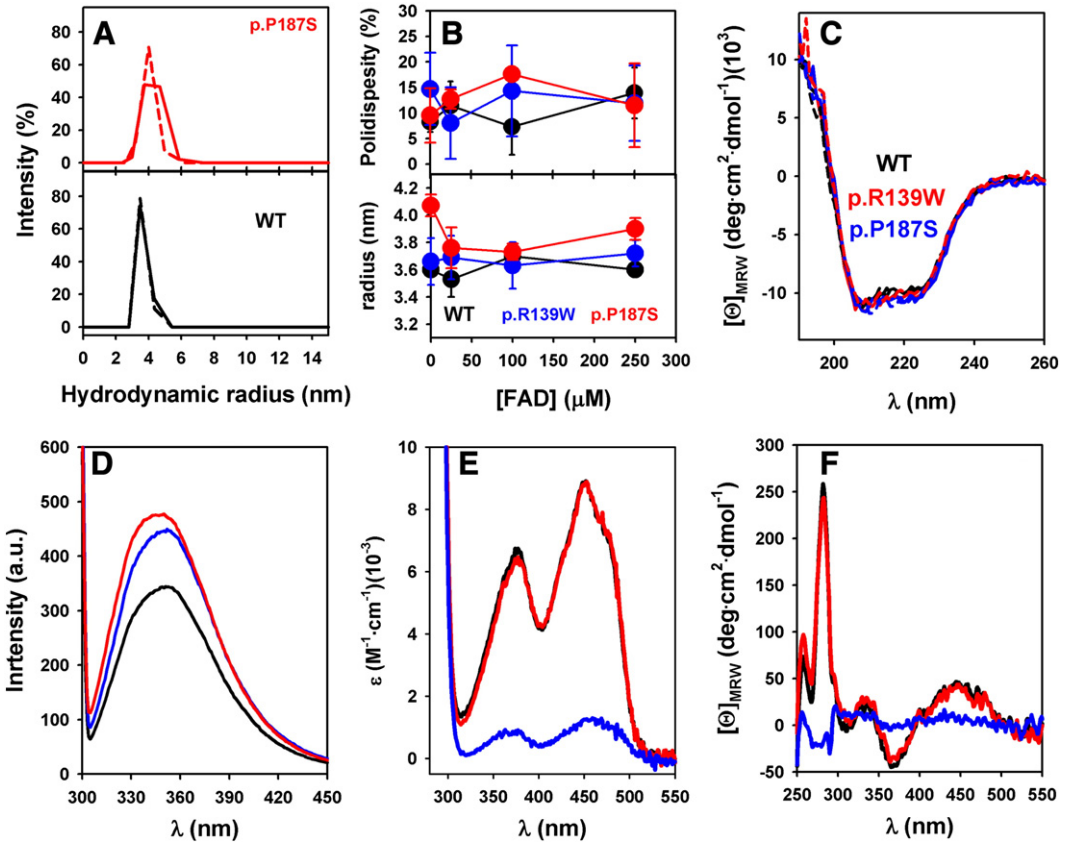

Fig. 3. Conformational properties and FAD binding to NQO1 enzymes. (A) Representative profiles of intensity vs. hydrodynamic radius for wild-type and p.P187S in the absence (solid line) and presence of 250 μM FAD; (B) Values of polydispersity and hydrodynamic radius as function of added FAD; data are mean ± s.d. from three independent experiments; (C) Far-UV CD spectra at 5 μM protein monomer in the absence (solid lines) and presence of 50 μM FAD (dashed lines); D) Trp fluorescence emission spectra ($\lambda_{exc} = 295$ nm); E and F) Absorption (E) and CD (F) Near-UV/visible spectra without adding extra FAD (FAD must not be added because it may give a signal also as free FAD). In all panels, the colour code is wild-type (black), p.R139W (red) and p.P187S (blue). In panels C–F, data are from single measurements.

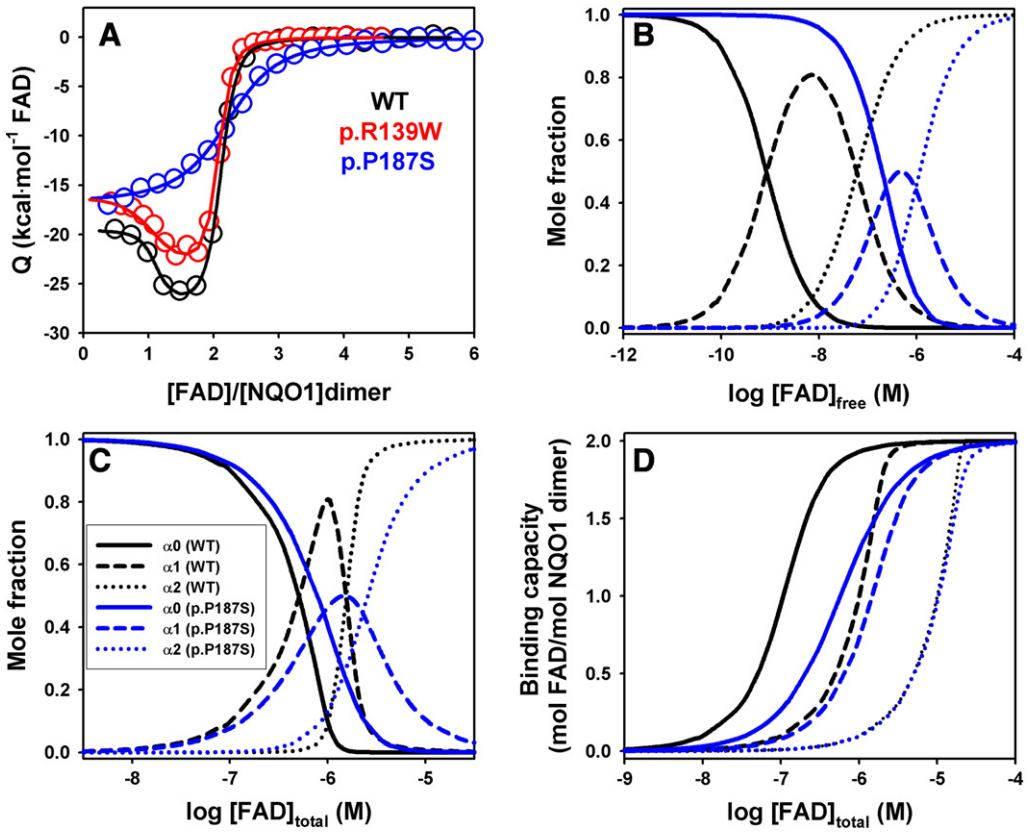

Fig. 4. Titration of NQO1 variants with FAD and ligand binding analyses by a binding polynomial formalism. (A) Binding isotherms of NQO1 enzymes (5–6 μM in dimer) titrated with FAD. Lines are best-fits to a sequential binding mechanism (wild-type and p.R139W) and a one independent and identical type of sites (p.P187S). Data are representative from two independent titrations. (B and C) Dependence of the mole fraction for different ligation species (solid line: α0, dimer with no FAD bound; dashed line: α1, dimer with 1 FAD bound; dotted line, α2, dimer with 2 FAD bound) for wild-type (black lines) and p.P187S (blue lines) on free (B) and total (C) FAD concentrations for 1 μM NQO1 dimer. (D) Dependence of the binding capacity (number of FAD molecules bound per NQO1 dimer) on the total FAD concentration for 0.1 (solid lines), 1 (dashed lines) and 10 (dotted lines) μM NQO1 dimers. Black lines are for wild-type and blue lines for p.P187S.

The melting temperatures of wild-type NQO1 and of each variant enzyme as determined by DSF were 50.6 ± 0.2 °C, 49.3 ± 0.2 °C and 43.3 ± 0.9 °C for 2 μM wild-type dimer, 2 μM p.R139W dimer (2 μM dimer) and 10 μM p.P187S dimer respectively (means of three independent determinations ± standard deviation; Fig. 5B). The T_m values for wild-type NQO1 and p.R139W can be compared directly since their concentrations were equal; there was a slight, but significant, thermal destabilization of the enzyme ($p = 0.0007$; t-test). It was not possible to measure the melting temperature of p.P187S at a concentration of 2 μM protein, presumably due to the low level of bound FAD which gives rise to the fluorescence signal in the assay. p.P187S showed a concentration dependent melting temperature: at 20 μM (dimer) it had a T_m of 47.6 ± 0.3 °C and at 10 μM the T_m was 43.3 ± 0.9 °C. This suggests that if it was possible to measure a melting temperature at 2 μM protein, it would be even lower than that recorded at 10 μM. Thus, this protein is, by far, the most thermally unstable of the three studied here. Susceptibility to limited proteolysis by trypsin increased in the order wild-type NQO1, p.R139W and p.P187S (Fig. 5C). This mirrors the pattern observed in the enzymes' melting temperatures.

3.5. Thermal stability and FAD binding

Thermal stability of NQO1 was studied in depth by differential scanning calorimetry (Fig. 6) and far-UV CD spectroscopy (Supplementary Fig. S4). By both techniques, we observed a single thermal transition, with the polymorphisms reducing T_m values by ~2 K (p.R139W) and ~8 K (p.P187S) (Fig. 6A, Supplementary Fig. S4; Table 3). The decrease in thermal stability by p.P187S agreed well with previous thermal inactivation assays [19] and our DSF experiments (Fig. 5B). Thermal denaturation of NQO1 variants was irreversible (Fig. 6B), and scan rate

Table 2
Thermodynamic parameters for the binding of FAD to NQO1 variants. Data are the mean from two independent titrations.

Sequential binding (two sites)						
	K_1 (M^{-1})	ΔH_1 (kcal · mol^{-1})	ΔS_1 (cal · mol^{-1} · K^{-1})	K_2 (M^{-1})	ΔH_1 (kcal · mol^{-1})	ΔS_1 (cal · mol^{-1} · K^{-1})
Wild-type	~$1.1 \cdot 10^9$	−19.2	−23.1	$1.7 \cdot 10^7$	−25.5	−52.4
p.R139W	~$3 \cdot 10^8$	−16.4	−16.5	$1.4 \cdot 10^7$	−23.7	−46.7
p.P187S	$5.5 \cdot 10^6$	−18.0	−29.4	$1.1 \cdot 10^6$	−16.0	−21.2

Identical, independent type of sites				
	N	K (M^{-1})	ΔH (kcal · mol^{-1})	ΔS (cal · mol^{-1} · K^{-1})
p.P187S	2.0	$2.1 \cdot 10^6$	−17.3	−29.0

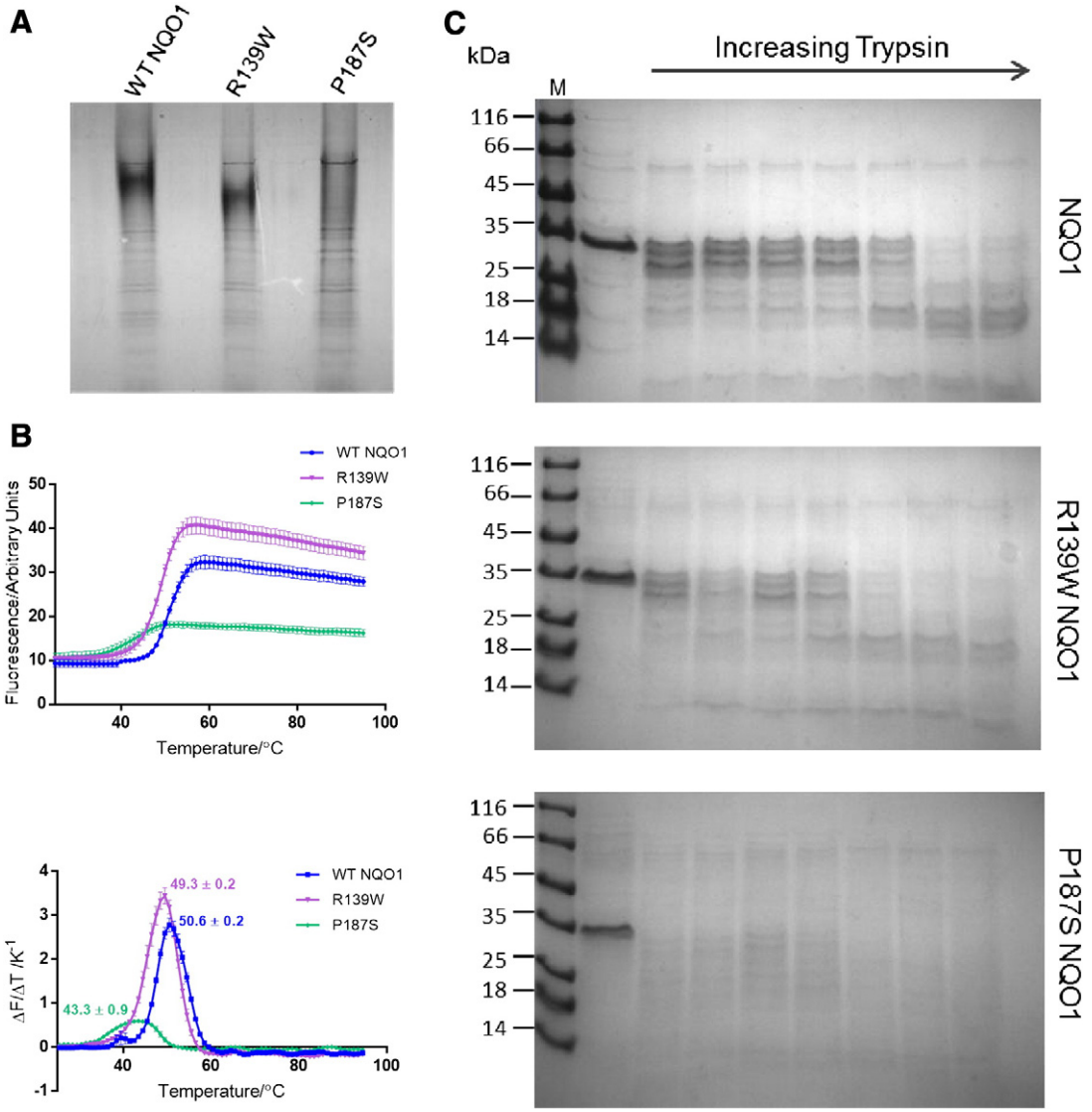

Fig. 5. Stability of NQO1 variants. (A) Tris–glycine native PAGE: 3 μM dimer of each protein was electrophoresed on a 10% gel at pH 8.8. (B) Differential scanning fluorimetry: thermal melt comparison for wild-type NQO1, p.R139W and p.P187S triplicate samples of wild-type NQO1 (2 μM dimer), p.R139W (2 μM dimer) and p.P187S (10 μM dimer) in HEPES–OH, pH 7.33 were subjected to an increase in temperature from 25 °C to 95 °C in 1 K increments with excitation at 460 nm and emission measured at 510 nm throughout thereby exploiting the fluorescence of the cofactor, FAD. Upper panel: the fluorescence emitted throughout the experiment; Lower panel: the first derivative of this fluorescence emission graph plotted against temperature. (C) Limited proteolysis by trypsin. Protein samples (3.5 μM dimer) with increasing concentrations of trypsin: 0, 9, 36, 63, 90, 360, 630, and 900 nM. Trypsin was dissolved in buffer R supplemented with 2 mM $CaCl_2$. Results are representative of three independent experiments.

(Fig. 6C) and protein concentration dependent (Fig. 6D), indicating that their denaturation is kinetically-controlled and is likely to involve dissociation of native NQO1 dimers prior to the rate-limiting denaturation step [54–56]. Despite the heterogeneous mixture of species in the native state ensemble (with different degrees of saturation of the NQO1 dimers with FAD), we tentatively analyzed the DSC profiles using the simplest model that may account for their behaviour, a two-state irreversible model with non-first order kinetics (Scheme 1). This model reproduced the experimental DSC scans well (Fig. 6A), yielding consistent parameters for thermal denaturation (E_a and ΔH values), and thus, it seems to be a reasonable description of the thermal denaturation of NQO1 (Table 3). Moreover, the model includes μ as a fitting parameter (where 1/μ is the reaction order), which allows the estimation of the reaction order from the shape of thermal scan [56]: when it is close to 1, the process is protein concentration independent (i.e. first-order), while a value close to 2 means that the process is protein concentration dependent and involves dissociation of NQO1 dimers prior to the rate-limiting denaturation step. Indeed, we obtain values of μ very close to 2 for wild-type and p.R139W, and somewhat lower for p.P187S, indicating dimer dissociation upon thermal denaturation for all three variants.

We then obtained NQO1 variants in their apo-form and studied their stability by DSC. Removal of FAD bound has little effect on the T_m values (Table 2). The model used to describe thermal denaturation of NQO1 enzymes as purified also seems to be applicable to the apo-forms (Table 3). An interesting result found is that apo-NQO1 wild-type and p.R139W enthalpy changes are much lower than those found for these variants as purified. The T_m dependence of ΔH values shows a linear dependence of 3.9 ± 0.5 kcal · mol^{-1} · K^{-1}, which is very close to the theoretical value for a protein of this size (3.8 kcal · mol^{-1} · K^{-1}) based on [60] (Fig. 6G). This result has two implications: first all apo-forms are expected to be natively folded (even though p.P187S seems to be more prone to form partially unfolded states, see [19] and Figs. 3A, 5A,C); second the higher ΔH values for wild-type and p.R139W as purified may arise from the dissociation of FAD, which shows binding enthalpies of 20–25 kcal · mol^{-1} (Table 2).

We also investigated the possible effect of FAD on the thermal stability of NQO1 variants (Fig. 6E,F; Supplementary Fig. S4B). Addition of

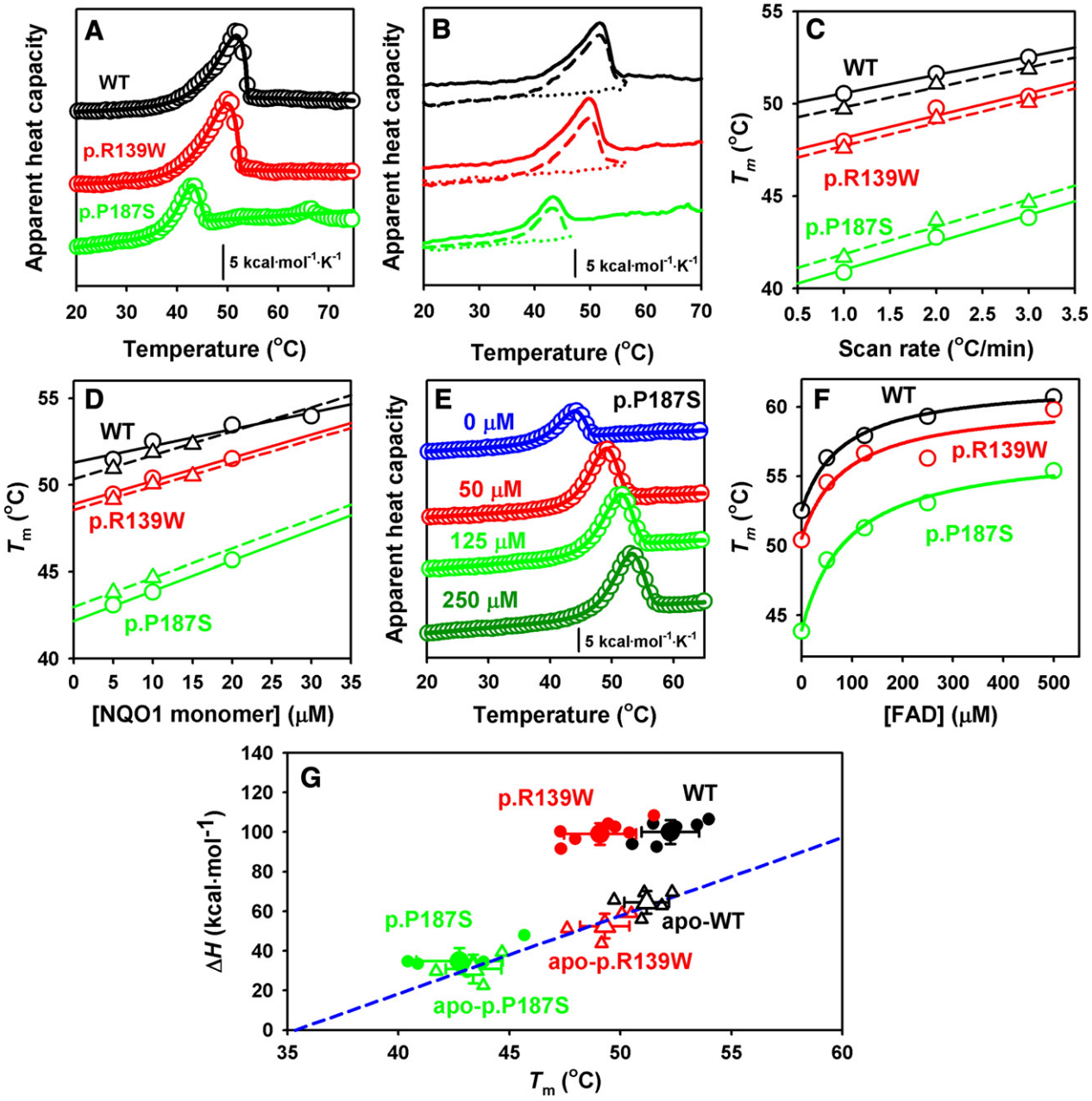

Fig. 6. DSC profiles of NQO1 variants. (A) DSC scan at 2 K/min and 10 μM monomer NQO1. Lines are best-fits to a two-state irreversible model with non-first order kinetics. (B) Irreversibility of thermal denaturation. The solid lines are scans up to 80 °C, dashed lines first-scans to a temperature close to the completion of the transition, and dotted lines are second-scans upon cooling down to 5 °C. Performed at 3 K/min and 5 μM monomer NQO1. (C) Scan rate dependence of the T_m values. Performed at 10 μM monomer NQO1. (D) Protein concentration dependence of T_m values. Performed at 3 K/min. (E) DSC profiles of p.P187S in the presence of different FAD concentrations. Lines are best-fits to a two-state irreversible model with non-first order kinetics. Performed at 3 K/min and 10 μM monomer NQO1. (F) Dependence of the T_m values on FAD concentration. Performed at 3 K/min and 10 μM monomer NQO1. (G) Denaturation enthalpies of NQO1 enzymes and structure–energetic correlations. Values from single scans are shown as small symbols, while large symbols are the mean ± s.d. Closed circles are for NQO1 enzymes as purified, and open triangles for apo NQO1 enzymes (panels c, d, g). The blue line is the linear fit of the data for apo-proteins providing a slope (ΔC_p) of 3.9 ± 0.5 kcal · mol^{-1} which agrees excellently with the theoretical value of 3.8 kcal · mol^{-1} from the parameterization of [60] for a folded protein of this size based on the number of residues. Note that the enthalpy values for NQO1 WT and p.R139W are ~40 kcal · mol^{-1} higher than those found for their apo-NQO1 forms, probably due to the contribution of FAD release upon denaturation. In panels C, D, F and G, the values displayed for single experiments are best-fit values to the two-state kinetic model (equations 1–3 in Supplementary data) and fitting errors are <0.1 °C (for T_m values) and <3 kcal · mol^{-1} (for ΔH values).

FAD increased the T_m values for all three variants in a concentration dependent manner; this was somewhat stronger for p.P187S. This result is not unexpected, since the p.P187S has the lowest occupancy of FAD binding sites in the absence of added FAD (Fig. 3E,F and [19]) and also lower affinity for this ligand [1] (Table 2). Since thermal denaturation of NQO1 is kinetically controlled, these results support the hypothesis that FAD kinetically stabilizes the NQO1 dimers thus increasing their denaturation half-lives, which is consistent with FAD binding at the dimer interface (Fig. 1; [5,61]).

3.6. Quantitative estimation of changes in kinetic stability by polymorphisms and FAD binding

To address, directly, the effect of polymorphisms on the kinetic stability of NQO1 as well as the stabilizing effect of FAD on them, we performed isothermal kinetic denaturation studies by Far-UV CD spectroscopy (Fig. 7). To compare the three variants, we chose 37 °C and 42 °C because they allow determination of kinetic stability in a time window of several minutes to hours, and the results

Table 3
Energetic parameters for thermal denaturation of NQO1 enzymes.

NQO1 variant	T_m (°C)[a]	ΔH (kcal · mol^{-1})[b,c]	E_a (kcal · mol^{-1})[b]	μ[b,c]
Wild-type	52.51 ± 0.06	100.1 ± 6.0	44.3 ± 5.8	2.6 ± 0.5
(apo)	(51.87 ± 0.03)	(64.5 ± 5.6)	(67.2 ± 9.6)	(1.9 ± 0.4)
p.R139W	50.39 ± 0.04	99.4 ± 5.6	48.9 ± 5.5	2.0 ± 0.3
(apo)	(50.07 ± 0.02)	(52.7 ± 6.3)	(80.7 ± 4.2)	(1.5 ± 0.1)
p.P178S	43.83 ± 0.02	32.7 ± 2.2	82.8 ± 4.5	1.4 ± 0.1
(apo)	(44.55 ± 0.02)	(30.9 ± 6.2)	(94.6 ± 6.2)	(1.2 ± 0.1)

[a] At 3 K/min and 10 μM in monomer. Data are from single experiments and errors are from fittings to a two-state kinetic model (equations 1–3 in Supplementary text).
[b] Mean ± s.d. from six five different experiments at different scan rates (1–3 K/min) and protein concentrations (5–30 μM in monomer).
[c] Expressed per NQO1 monomer.

obtained can be considered as biologically relevant. The apparent half-lives were estimated at 3.5 μM monomer by fitting to a single exponential function. In the absence of added FAD, the kinetic stability of NQO1 is reduced by ~7-fold and ~70-fold in p.R139W and p.P187S respectively at both 37 °C and 42 °C (Fig. 7A,B). At 37 °C the half-life for denaturation is 9 min, 1.5 h and 9 h for p.P187S, p.R139W and wild-type NQO1 (Fig. 7A), while their stability is about 6-fold lower at 42 °C (Fig. 7B). Addition of FAD increased the kinetic stability of the variants remarkably (Fig. 7C,D). Indeed, p.R139W and p.P187S reached the wild-type (as purified) level of kinetic stability at concentrations of ~20 and ~250 μM of added FAD, respectively (Fig. 7D). Overall, our results show that the kinetic stability of p.P187S and p.R139W can be restored *in vitro* by addition of micromolar concentrations of FAD.

4. Discussion

Our data demonstrate that both cancer-associated variants are destabilized compared to the wild-type protein *in vitro*; p.P187S is substantially more affected than p.R139W. Kinetic destabilization is overcome by addition of FAD in a concentration dependent manner, and this stabilization still increases at concentrations much higher than the K_d values for FAD, as seen by DSC thermal scan and kinetic denaturation studies by CD. This behaviour is a consequence of the kinetically controlled nature of NQO1 denaturation. FAD mediated stabilization occurs even at concentrations of ligand at which the enzyme is close to be saturated possibly by reducing the fraction of unligated (no FAD bound) species *kinetically sensitive* to denaturation (see [56,62] for a detailed discussion of these kinetic models). Importantly, our *in vitro* stability analyses mirror the intracellular behaviour of p.P187S. In the absence of an exogenous supply of FAD, this variant is very unstable due to rapid proteasomal degradation, while addition of FAD (by riboflavin supplementation) increases the resistance towards proteasomal degradation in a concentration dependent manner [19,32]. Therefore, the *in vitro* and the intracellular instabilities of p.P187S are likely to have a common origin in the low thermodynamic stability of its apo-form and the low affinity of this variant for FAD. In turn, increasing FAD saturation may boost p.P187S stability by shifting the equilibrium towards the holo-form, and also enhance specific activity by overcoming the affinity defect of this variant for FAD. Our results also suggest a similar scenario for p.R139W, although in this case, we expect a less dramatic decrease in intracellular stability and a higher specific activity in the absence of FAD (or riboflavin) supplementation.

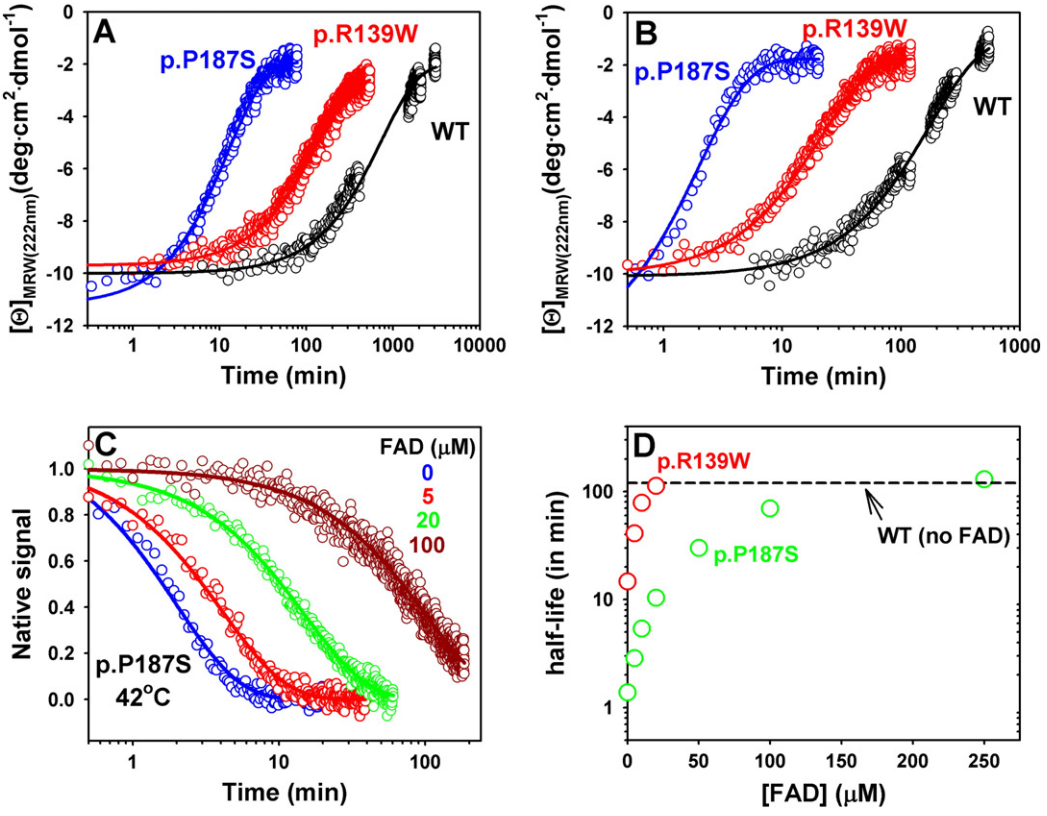

Fig. 7. Kinetic denaturation studies by CD spectroscopy. (A and B) Kinetic traces for denaturation of NQO1 variants without added FAD at 37 °C (A) and 42 °C (B). (C) Kinetic traces for p.P187S in the presence of different FAD concentrations at 42 °C. In panels A–C, lines are best fits to a single exponential function. (D) FAD concentration dependence of the apparent denaturation half-life of p.R139W and p.P187S at 42 °C. For sake of comparison, the denaturation half-life for wild-type at this temperature without added FAD is shown as a horizontal dashed line. In panel D, data are best-fit values obtained from single experimental using a single exponential function, and fitting errors are lower than 10% of the best-value half life.

Previously, Moscovitz and coworkers were able to detect by mass spectrometry a population of partially unfolded states in apo-NQO1, while binding of FAD seems to shift the folding equilibrium towards the native dimer [19]. Our conformational and kinetic stability studies further support this study, and demonstrate that similar effects occur in p.P187S and p.R139W. The data of Moscovitz et al. show that partially folded states are populated at low levels in the native state ensemble (see the low intensities of the *partially unfolded* vs. *folded* peaks in Fig. 2 of [19]), and thus, they do not largely perturb the averaged molecular properties reported by us here. When corrected for the contribution of FAD binding, the denaturation enthalpies of all (apo-)NQO1 variants at their T_m are consistent with a folded native state based on well-known structure-energetics parameterizations (see Fig. 5G), indicating that departures from the folded state (i.e. the partially unfolded states reported by Moscovitz et al. [19]) are marginal. Nevertheless, since these partially unfolded states may be more prone to aggregation and degradation than the native state, they may be critical to determine the kinetic stability *in vitro* (our work) and in cells [19]. By simply assuming that FAD binds and selectively stabilizes the native state, the partially unfolded states will be poorly populated in the holo-state, consistent with the results obtained by Moscovitz et al. using mass spectrometry [19] and our thermal and kinetic stability studies. Thus, FAD binding may enhance NQO1 activity by increasing the thermodynamic stability of the folded dimer under native conditions. Interestingly, Oliveberg and coworkers have shown that binding of copper and zinc ions to apo-SOD provides a larger thermodynamic stabilization than the sum of dimerization and monomer unfolding in the apo-state [63].

Since p.R139W has comparable kinetic constants to wild-type NQO1, the explanation for its different behaviour *in vivo* may lie in its activity towards its natural electron acceptor substrates. Previously, p.R139W has been shown to have a higher K_m value for DCPIP but the same K_m value for menadione; it also has a 60% lower activity in the reduction of mitomycin C (MMC) [45]. Therefore, p.R139W may have much higher K_m values and/or lower k_{cat} values for quinone substrates *in vivo*. Its slightly decreased stability compared to wild-type NQO1 may also be a factor. This variant may also be less effective at stabilizing p53; irradiation-induced expression of p53 has been shown to be attenuated in cells expressing p.R139W [46]. Interestingly, in the structurally related enzyme NQO2, *reduced* oxidoreductase activity resulting from a common polymorphism (rs1143684; p.F47L) is associated with improved prognosis in some cancers [64–66]. This suggests that, despite structural and catalytic similarities between the two enzymes, their roles in the cell have important differences.

As demonstrated here, the stability and oxidoreductase activity of p.P187S recover in the presence of excess FAD. Recent studies on human cells which express this form of NQO1 have shown that supplementation of the cell growth media with the FAD precursor riboflavin causes stabilization of p.P187S, leading to increased levels in the cells and increased NQO1 activity [19]. Taken together, this suggests that dietary supplementation with riboflavin-rich foods may be advisable for individuals with the p.P187S and p.R139W polymorphisms, especially those who are homozygous. This therapy resembles those used for different inborn errors of metabolism caused by protein instability, and based on vitamin and/or cofactor supplementation, some of which involve FAD-dependent enzymes [67–71]. Furthermore, our results predict that the levels of vitamin B2 required to rescue p.R139W will be lower than those required for p.P187S (see Fig. 7). Alternatively a "pharmacological chaperone" approach could be taken which would require the identification of a small molecule which would specifically and kinetically stabilise p.P187S and p.R139W, an approach previously shown to be successful in conformational metabolic diseases [68,72,73]. Some of the methods for studying NQO1 stability described here, most notably DSF and DSC, may prove valuable in screening for and characterizing such compounds.

Supplementary data to this article can be found online at http://dx.doi.org/10.1016/j.bbadis.2014.08.011.

Acknowledgements

We thank Dr. Jose Manuel Sanchez-Ruiz for his support. We also thank Dr. Francisco Conejero-Lara for access to the DLS instrument and Prof. Aaron Maule for access to the qPCR machine used for DSF experiments. ALP acknowledges support from MINECO (grants CSD2009-00088 and BIO2012-34937), Junta de Andalucia (grant CTS-11-07187) and FEDER Funds. ALP is a recipient of a Ramon y Cajal contract from MINECO (RYC2009-04147). CFM thanks the Department of Employment and Learning, Northern Ireland (DELNI) for a PhD studentship.

References

[1] S. Chen, K. Wu, R. Knox, Structure–function studies of DT-diaphorase (NQO1) and NRH:quinone oxidoreductase (NQO2), Free Radic. Biol. Med. 29 (2000) 276–284.
[2] L. Ernster, L. Danielson, M. Ljunggren, DT diaphorase. I. Purification from the soluble fraction of rat-liver cytoplasm, and properties, Biochim. Biophys. Acta 58 (1962) 171–188.
[3] C. Lind, E. Cadenas, P. Hochstein, L. Ernster, DT-diaphorase: purification, properties, and function, Methods Enzymol. 186 (1990) 287–301.
[4] M. Faig, M.A. Bianchet, P. Talalay, S. Chen, S. Winski, D. Ross, L.M. Amzel, Structures of recombinant human and mouse NAD(P)H:quinone oxidoreductases: species comparison and structural changes with substrate binding and release, Proc. Natl. Acad. Sci. U. S. A. 97 (2000) 3177–3182.
[5] G. Asher, O. Dym, P. Tsvetkov, J. Adler, Y. Shaul, The crystal structure of NAD(P)H quinone oxidoreductase 1 in complex with its potent inhibitor dicoumarol, Biochemistry 45 (2006) 6372–6378.
[6] L. Buryanovskyy, Y. Fu, M. Boyd, Y. Ma, T.C. Hsieh, J.M. Wu, Z. Zhang, Crystal structure of quinone reductase 2 in complex with resveratrol, Biochemistry 43 (2004) 11417–11426.
[7] M.A. Adams, Z. Jia, Modulator of drug activity B from *Escherichia coli*: crystal structure of a prokaryotic homologue of DT-diaphorase, J. Mol. Biol. 359 (2006) 455–465.
[8] S. Hosoda, W. Nakamura, K. Hayashi, Properties and reaction mechanism of DT diaphorase from rat liver, J. Biol. Chem. 249 (1974) 6416–6423.
[9] J.J. Kwiek, T.A. Haystead, J. Rudolph, Kinetic mechanism of quinone oxidoreductase 2 and its inhibition by the antimalarial quinolines, Biochemistry 43 (2004) 4538–4547.
[10] J.K. Tie, D.Y. Jin, D.L. Straight, D.W. Stafford, Functional study of the vitamin K cycle in mammalian cells, Blood 117 (2011) 2967–2974.
[11] B.O. Ingram, J.L. Turbyfill, P.J. Bledsoe, A.K. Jaiswal, D.W. Stafford, Assessment of the contribution of NAD(P)H-dependent quinone oxidoreductase 1 (NQO1) to the reduction of vitamin K in wild-type and NQO1-deficient mice, Biochem. J. 456 (2013) 47–54.
[12] D. Ross, J.K. Kepa, S.L. Winski, H.D. Beall, A. Anwar, D. Siegel, NAD(P)H:quinone oxidoreductase 1 (NQO1): chemoprotection, bioactivation, gene regulation and genetic polymorphisms, Chem. Biol. Interact. 129 (2000) 77–97.
[13] D. Siegel, E.M. Bolton, J.A. Burr, D.C. Liebler, D. Ross, The reduction of α-tocopherol quinone by human NAD(P)H:quinone oxidoreductase: the role of alpha-tocopherol hydroquinone as a cellular antioxidant, Mol. Pharmacol. 52 (1997) 300–305.
[14] C. Lind, P. Hochstein, L. Ernster, DT-diaphorase as a quinone reductase: a cellular control device against semiquinone and superoxide radical formation, Arch. Biochem. Biophys. 216 (1982) 178–185.
[15] G. Asher, J. Lotem, B. Cohen, L. Sachs, Y. Shaul, Regulation of p53 stability and p53-dependent apoptosis by NADH quinone oxidoreductase 1, Proc. Natl. Acad. Sci. U. S. A. 98 (2001) 1188–1193.
[16] G. Asher, J. Lotem, R. Kama, L. Sachs, Y. Shaul, NQO1 stabilizes p53 through a distinct pathway, Proc. Natl. Acad. Sci. U. S. A. 99 (2002) 3099–3104.
[17] G. Asher, Z. Bercovich, P. Tsvetkov, Y. Shaul, C. Kahana, 20S proteasomal degradation of ornithine decarboxylase is regulated by NQO1, Mol. Cell 17 (2005) 645–655.
[18] G. Asher, P. Tsvetkov, C. Kahana, Y. Shaul, A mechanism of ubiquitin-independent proteasomal degradation of the tumor suppressors p53 and p73, Genes Dev. 19 (2005) 316–321.
[19] O. Moscovitz, P. Tsvetkov, N. Hazan, I. Michaelevski, H. Keisar, G. Ben-Nissan, Y. Shaul, M. Sharon, A mutually inhibitory feedback loop between the 20S proteasome and its regulator, NQO1, Mol. Cell 47 (2012) 76–86.
[20] M. Belinsky, A.K. Jaiswal, NAD(P)H:quinone oxidoreductase1 (DT-diaphorase) expression in normal and tumor tissues, Cancer Metastasis Rev. 12 (1993) 103–117.
[21] P. Reigan, M.A. Colucci, D. Siegel, A. Chilloux, C.J. Moody, D. Ross, Development of indolequinone mechanism-based inhibitors of NAD(P)H:quinone oxidoreductase 1 (NQO1): NQO1 inhibition and growth inhibitory activity in human pancreatic MIA PaCa-2 cancer cells, Biochemistry 46 (2007) 5941–5950.
[22] K.A. Nolan, H. Zhao, P.F. Faulder, A.D. Frenkel, D.J. Timson, D. Siegel, D. Ross, T.R. Burke Jr., I.J. Stratford, R.A. Bryce, Coumarin-based inhibitors of human NAD(P)H:quinone oxidoreductase-1. Identification, structure–activity, off-target effects and in vitro human pancreatic cancer toxicity, J. Med. Chem. 50 (2007) 6316–6325.
[23] K.A. Nolan, K.A. Scott, J. Barnes, J. Doncaster, R.C. Whitehead, I.J. Stratford, Pharmacological inhibitors of NAD(P)H quinone oxidoreductase, NQO1: structure/activity relationships and functional activity in tumour cells, Biochem. Pharmacol. 80 (2010) 977–981.

[24] K.A. Scott, J. Barnes, R.C. Whitehead, I.J. Stratford, K.A. Nolan, Inhibitors of NQO1: identification of compounds more potent than dicoumarol without associated off-target effects, Biochem. Pharmacol. 81 (2011) 355–363.
[25] S.M. Bailey, M.D. Wyatt, F. Friedlos, J.A. Hartley, R.J. Knox, A.D. Lewis, P. Workman, Involvement of DT-diaphorase (EC 1.6.99.2) in the DNA cross-linking and sequence selectivity of the bioreductive anti-tumour agent EO9, Br. J. Cancer 76 (1997) 1596–1603.
[26] S.M. Bailey, A.D. Lewis, R.J. Knox, L.H. Patterson, G.R. Fisher, P. Workman, Reduction of the indoloquinone anticancer drug EO9 by purified DT-diaphorase: a detailed kinetic study and analysis of metabolites, Biochem. Pharmacol. 56 (1998) 613–621.
[27] D. Siegel, H. Beall, C. Senekowitsch, M. Kasai, H. Arai, N.W. Gibson, D. Ross, Bioreductive activation of mitomycin C by DT-diaphorase, Biochemistry 31 (1992) 7879–7885.
[28] R.D. Traver, T. Horikoshi, K.D. Danenberg, T.H. Stadlbauer, P.V. Danenberg, D. Ross, N. W. Gibson, NAD(P)H:quinone oxidoreductase gene expression in human colon carcinoma cells: characterization of a mutation which modulates DT-diaphorase activity and mitomycin sensitivity, Cancer Res. 52 (1992) 797–802.
[29] R.D. Traver, D. Siegel, H.D. Beall, R.M. Phillips, N.W. Gibson, W.A. Franklin, D. Ross, Characterization of a polymorphism in NAD(P)H:quinone oxidoreductase (DT-diaphorase), Br. J. Cancer 75 (1997) 69–75.
[30] P. Flicek, I. Ahmed, M.R. Amode, D. Barrell, K. Beal, S. Brent, D. Carvalho-Silva, P. Clapham, G. Coates, S. Fairley, S. Fitzgerald, L. Gil, C. Garcia-Giron, L. Gordon, T. Hourlier, S. Hunt, T. Juettemann, A.K. Kahari, S. Keenan, M. Komorowska, E. Kulesha, I. Longden, T. Maurel, W.M. McLaren, M. Muffato, R. Nag, B. Overduin, M. Pignatelli, B. Pritchard, E. Pritchard, H.S. Riat, G.R. Ritchie, M. Ruffier, M. Schuster, D. Sheppard, D. Sobral, K. Taylor, A. Thormann, S. Trevanion, S. White, S.P. Wilder, B.L. Aken, E. Birney, F. Cunningham, I. Dunham, J. Harrow, J. Herrero, T.J. Hubbard, N. Johnson, R. Kinsella, A. Parker, G. Spudich, A. Yates, A. Zadissa, S.M. Searle, Ensembl 2013, Nucleic Acids Res. 41 (2013) D48–D55.
[31] D. Siegel, S.M. McGuinness, S.L. Winski, D. Ross, Genotype–phenotype relationships in studies of a polymorphism in NAD(P)H:quinone oxidoreductase 1, Pharmacogenetics 9 (1999) 113–121.
[32] D. Siegel, A. Anwar, S.L. Winski, J.K. Kepa, K.L. Zolman, D. Ross, Rapid polyubiquitination and proteasomal degradation of a mutant form of NAD(P)H:quinone oxidoreductase 1, Mol. Pharmacol. 59 (2001) 263–268.
[33] W.G. Hu, J.J. Hu, W. Cai, M.H. Zheng, L. Zang, Z.T. Wang, Z.G. Zhu, The NAD(P)H: quinine oxidoreductase 1 (NQO1) gene 609 C>T polymorphism is associated with gastric cancer risk: evidence from a case–control study and a meta-analysis, Asian Pac. J. Cancer Prev. 15 (2014) 2363–2367.
[34] C. Li, Y. Zhou, Association between NQO1 C609T polymorphism and acute lymphoblastic leukemia risk: evidence from an updated meta-analysis based on 17 case–control studies, J. Cancer Res. Clin. Oncol. 140 (2014) 873–881.
[35] J. Yin, L. Wang, X. Wang, L. Zheng, Y. Shi, A. Shao, W. Tang, G. Ding, C. Liu, R. Liu, S. Chen, H. Gu, NQO1 rs1800566 C>T polymorphism was associated with a decreased risk of esophageal cancer in a Chinese population, Scand. J. Gastroenterol. 49 (2014) 317–322.
[36] K. Liu, H. Tian, K.Z. Yu, W.Y. Shen, Z.C. Mao, C.H. Jin, H.B. Pan, J.X. He, Association between NQO1 Pro187Ser polymorphism and esophageal cancer: a meta-analysis, Tumour Biol. 35 (2014) 2063–2068.
[37] H. Zhao, F. Zhu, J. Sun, X. Meng, Meta-analysis of the association between NQO1 Pro187Ser polymorphism and colorectal cancer in Asians, Tumour Biol. 35 (2014) 2111–2116.
[38] B. Lajin, A. Alachkar, The NQO1 polymorphism C609T (Pro187Ser) and cancer susceptibility: a comprehensive meta-analysis, Br. J. Cancer 109 (2013) 1325–1337.
[39] E.A. Rosvold, K.A. McGlynn, E.D. Lustbader, K.H. Buetow, Identification of an NAD(P) H:quinone oxidoreductase polymorphism and its association with lung cancer and smoking, Pharmacogenetics 5 (1995) 199–206.
[40] L.L. Xu, J.C. Wain, D.P. Miller, S.W. Thurston, L. Su, T.J. Lynch, D.C. Christiani, The NAD(P)H:quinone oxidoreductase 1 gene polymorphism and lung cancer: differential susceptibility based on smoking behavior, Cancer Epidemiol. Biomarkers Prev. 10 (2001) 303–309.
[41] N. Rothman, M.T. Smith, R.B. Hayes, R.D. Traver, B. Hoener, S. Campleman, G.L. Li, M. Dosemeci, M. Linet, L. Zhang, L. Xi, S. Wacholder, W. Lu, K.B. Meyer, N. Titenko-Holland, J.T. Stewart, S. Yin, D. Ross, Benzene poisoning, a risk factor for hematological malignancy, is associated with the NQO1 609C → T mutation and rapid fractional excretion of chlorzoxazone, Cancer Res. 57 (1997) 2839–2842.
[42] J.L. Moran, D. Siegel, D. Ross, A potential mechanism underlying the increased susceptibility of individuals with a polymorphism in NAD(P)H:quinone oxidoreductase 1 (NQO1) to benzene toxicity, Proc. Natl. Acad. Sci. U. S. A. 96 (1999) 8150–8155.
[43] D. Ross, Functions and distribution of NQO1 in human bone marrow: potential clues to benzene toxicity, Chem. Biol. Interact. 153–154 (2005) 137–146.
[44] L.T. Hu, J. Stamberg, S. Pan, The NAD(P)H:quinone oxidoreductase locus in human colon carcinoma HCT 116 cells resistant to mitomycin C, Cancer Res. 56 (1996) 5253–5259.
[45] S.S. Pan, G.L. Forrest, S.A. Akman, L.T. Hu, NAD(P)H:quinone oxidoreductase expression and mitomycin C resistance developed by human colon cancer HCT 116 cells, Cancer Res. 55 (1995) 330–335.
[46] M. Sato, M. Takagi, S. Mizutani, Irradiation-induced p53 expression is attenuated in cells with NQO1 C465T polymorphism, J. Med. Dent. Sci. 57 (2010) 139–145.
[47] M. Eguchi-Ishimae, M. Eguchi, E. Ishii, D. Knight, Y. Sadakane, K. Isoyama, H. Yabe, S. Mizutani, M. Greaves, The association of a distinctive allele of NAD(P)H:quinone oxidoreductase with pediatric acute lymphoblastic leukemias with MLL fusion genes in Japan, Haematologica 90 (2005) 1511–1515.
[48] G. Lennon, C. Auffray, M. Polymeropoulos, M.B. Soares, The I.M.A.G.E. Consortium: an integrated molecular analysis of genomes and their expression, Genomics 33 (1996) 151–152.
[49] W. Wang, B.A. Malcolm, Two-stage PCR protocol allowing introduction of multiple mutations, deletions and insertions using QuikChange site-directed mutagenesis, Biotechniques 26 (1999) 680–682.
[50] M.M. Bradford, A rapid and sensitive method for the quantitation of microgram quantities of protein utilizing the principle of protein–dye binding, Anal. Biochem. 72 (1976) 248–254.
[51] H. Schagger, Tricine-SDS-PAGE, Nat. Protoc. 1 (2006) 16–22.
[52] F. Forneris, R. Orru, D. Bonivento, L.R. Chiarelli, A. Mattevi, ThermoFAD, a thermofluor-adapted flavin *ad hoc* detection system for protein folding and ligand binding, FEBS J. 276 (2009) 2833–2840.
[53] C.F. Megarity, H.K. Looi, D.J. Timson, The *Saccharomyces cerevisiae* quinone oxidoreductase Lot6p: stability, inhibition and cooperativity, FEMS Yeast Res. 14 (2014) 797–807.
[54] N. Mesa-Torres, I. Fabelo-Rosa, D. Riverol, C. Yunta, A. Albert, E. Salido, A.L. Pey, The role of protein denaturation energetics and molecular chaperones in the aggregation and mistargeting of mutants causing primary hyperoxaluria type I, PLoS One 8 (2013) e71963.
[55] A.L. Pey, E. Salido, J.M. Sanchez-Ruiz, Role of low native state kinetic stability and interaction of partially unfolded states with molecular chaperones in the mitochondrial protein mistargeting associated with primary hyperoxaluria, Amino Acids 41 (2011) 1233–1245.
[56] J.M. Sanchez-Ruiz, Theoretical analysis of Lumry–Eyring models in differential scanning calorimetry, Biophys. J. 61 (1992) 921–935.
[57] A. Cornish-Bowden, Fundamentals of Enzyme Kinetics, Portland Press, London, 2004.
[58] B. Rase, T. Bartfai, L. Ernster, Purification of DT-diaphorase by affinity chromatography. Occurrence of two subunits and nonlinear Dixon and Scatchard plots of the inhibition by anticoagulants, Arch. Biochem. Biophys. 172 (1976) 380–386.
[59] S. Hustad, P.M. Ueland, J. Schneede, Quantification of riboflavin, flavin mononucleotide, and flavin adenine dinucleotide in human plasma by capillary electrophoresis and laser-induced fluorescence detection, Clin. Chem. 45 (1999) 862–868.
[60] A.D. Robertson, K.P. Murphy, Protein structure and the energetics of protein stability, Chem. Rev. 97 (1997) 1251–1268.
[61] R. Li, M.A. Bianchet, P. Talalay, L.M. Amzel, The three-dimensional structure of NAD(P)H:quinone reductase, a flavoprotein involved in cancer chemoprotection and chemotherapy: mechanism of the two-electron reduction, Proc. Natl. Acad. Sci. U. S. A. 92 (1995) 8846–8850.
[62] A.L. Pey, T. Majtan, J.M. Sanchez-Ruiz, J.P. Kraus, Human cystathionine β-synthase (CBS) contains two classes of binding sites for *S*-adenosylmethionine (SAM): complex regulation of CBS activity and stability by SAM, Biochem. J. 449 (2013) 109–121.
[63] A. Nordlund, M. Oliveberg, SOD1-associated ALS: a promising system for elucidating the origin of protein-misfolding disease, HFSP J. 2 (2008) 354–364.
[64] D. Jamieson, N. Cresti, J. Bray, J. Sludden, M.J. Griffin, N.M. Hawsawi, E. Famie, E.V. Mould, M.W. Verrill, F.E. May, A.V. Boddy, Two minor NQO1 and NQO2 alleles predict poor response of breast cancer patients to adjuvant doxorubicin and cyclophosphamide therapy, Pharmacogenet. Genomics 21 (2011) 808–819.
[65] M. Hubackova, R. Vaclavikova, M. Ehrlichova, M. Mrhalova, R. Kodet, K. Kubackova, D. Vrana, I. Gut, P. Soucek, Association of superoxide dismutases and NAD(P)H quinone oxidoreductases with prognosis of patients with breast carcinomas, Int. J. Cancer 130 (2012) 338–348.
[66] C.F. Megarity, J.R. Gill, M. Clare Caraher, I.J. Stratford, K.A. Nolan, D.J. Timson, The two common polymorphic forms of human NRH-quinone oxidoreductase 2 (NQO2) have different biochemical properties, FEBS Lett. 588 (2014) 1666–1672.
[67] J.V. Rodrigues, B.J. Henriques, T.G. Lucas, C.M. Gomes, Cofactors and metabolites as protein folding helpers in metabolic diseases, Curr. Top. Med. Chem. 12 (2012) 2546–2559.
[68] J. Underhaug, O. Aubi, A. Martinez, Phenylalanine hydroxylase misfolding and pharmacological chaperones, Curr. Top. Med. Chem. 12 (2012) 2534–2545.
[69] T.G. Lucas, B.J. Henriques, J.V. Rodrigues, P. Bross, N. Gregersen, C.M. Gomes, Cofactors and metabolites as potential stabilizers of mitochondrial acyl-CoA dehydrogenases, Biochim. Biophys. Acta 1812 (2011) 1658–1663.
[70] N. Cornelius, F.E. Frerman, T.J. Corydon, J. Palmfeldt, P. Bross, N. Gregersen, R.K. Olsen, Molecular mechanisms of riboflavin responsiveness in patients with ETF-QO variations and multiple acyl-CoA dehydrogenation deficiency, Hum. Mol. Genet. 21 (2012) 3435–3448.
[71] A.L. Pey, Protein homeostasis disorders of key enzymes of amino acids metabolism: mutation-induced protein kinetic destabilization and new therapeutic strategies, Amino Acids 45 (2013) 1331–1341.
[72] C.M. Gomes, Protein misfolding in disease and small molecule therapies, Curr. Top. Med. Chem. 12 (2012) 2460–2469.
[73] A. Jorge-Finnigan, S. Brasil, J. Underhaug, P. Ruiz-Sala, B. Merinero, R. Banerjee, L.R. Desviat, M. Ugarte, A. Martinez, B. Perez, Pharmacological chaperones as a potential therapeutic option in methylmalonic aciduria cblB type, Hum. Mol. Genet. 22 (2013) 3680–3689.